Inferring COVID-19 spreading rates and potential change points for case number forecasts

Jonas Dehning,[1†] Johannes Zierenberg,[1†] F. Paul Spitzner,[1†]
Michael Wibral,[2] Joao Pinheiro Neto,[1] Michael Wilczek,[1†]Viola Priesemann[1*]

[1] Max Planck Institute for Dynamics and Self-Organization, Göttingen, Germany,
[2] Campus Institute for Dynamics of Biological Networks, University Göttingen, Germany

*To whom correspondence should be addressed; E-mail: viola.priesemann@ds.mpg.de.
[†] Authors contributed equally

As COVID-19 is rapidly spreading across the globe, short-term modeling forecasts provide time-critical information for decisions on containment and mitigation strategies. A main challenge for short-term forecasts is the assessment of key epidemiological parameters and how they change as first governmental intervention measures are showing an effect. By combining an established epidemiological model with Bayesian inference, we analyze the time dependence of the effective growth rate of new infections. For the case of COVID-19 spreading in Germany, we detect change points in the effective growth rate which correlate well with the times of publicly announced interventions. We furthermore explore different scenarios based on the number of change points, which give indications about the impact of the wide-spread voluntary personal adaption and government-imposed mitigation strategies.

1 Introduction

During the initial outbreak of an epidemic, reliable short-term forecasts are key to estimate required medical capacities, and to inform and advice the public and the decision makers (*1*). During this initial phase, three tasks are of particular importance to provide time-critical information for crisis mitigation: (1) establishing central epidemiological parameters such as the basic reproduction number that can be used for short-term forecasting; (2) simulating the effects of different possible intervention measures aimed at mitigation of the outbreak; (3) estimating the actual effects of the measures taken to rapidly adjust them and to adapt short-term forecasts. Tackling these tasks is challenging due to the large statistical and systematic errors present during the initial stages of an epidemic with its low case numbers. Further complications arise from mitigation measures being taken rapidly, while the outbreak unfolds, but taking effect only after an unknown delay. To obtain sensible parameter estimates for short-term forecasting and policy evaluation despite these complications, any prior knowledge available needs to be integrated into modeling efforts to reduce uncertainties. This includes knowledge about basic mechanisms of disease transmission, recovery, as well as preliminary estimates of epidemiological parameters from other countries, or from closely related pathogens. The integration of prior knowledge, the quantitative assessment of the remaining uncertainties about epidemiological parameters, and the principled propagation of these uncertainties into forecasts is the domain of Bayesian modeling and inference.

Here, we draw on an established class of models for epidemic outbreaks: The Susceptible-Infected-Recovered (SIR) model (*2–5*) specifies the rates with which population compartments change over time, i.e., with which susceptible people become infectious, or infectious people recover. This simple model can be formulated in terms of coupled ordinary differential equations (in mean field), which enable analytical treatment (*6, 7*) or fast evaluation ideally suited for

Bayesian inference. Accordingly, SIR-like models have been used to model epidemic spreads, from detailed scenario discussions (*8–10*) to Bayesian Markov-Chain Monte Carlo parameter estimation (*11–13*). Recently, this family of models also played a dominant role in the analyses of the global COVID-19 outbreak, from scenario forecast (*14–17*) to inference (*18–20*).

We combine the SIR model with Bayesian parameter inference and augment the model by a time-varying spreading rate λ. The time-varying λ is implemented via potential change points reflecting changes in λ driven by governmental intervention measures. Based on three distinct measures taken in Germany, we also expect to find three corresponding change points. We already detect two such change points from reported COVID-19 case numbers. We find a clear decrease of the spreading rate λ from 0.41 (CI [0.34,0.49]) to 0.23 (CI [0.20,0.29]), with this decrease initiated around March 7th (CI [4th,10th]), and a second decrease down to 0.13 (CI [0.10,0.17]) initiated around March 16th (CI [15th,18th]). This matches the timing of the first two governmental mitigation measures, i.e. first the cancellation of large public events such as trade fairs and soccer matches, and second the closing of schools, child-care facilities, and non-essential shops. We expect a further change point because a third, more stringent lock-down measure was introduced in the following week (March 22nd). However, at present case data do not provide the necessary information on the strength of that third change in λ due to the delay between infection and report of the confirmed case of about 10 days. In a situation like this where we know that a change in the spreading rate λ has happened but its effect is unobservable yet, forecasts are necessarily difficult.

Our framework can help to infer the effectiveness of past measures as well as to explore potential future scenarios with propagating the respective uncertainties. It can be readily adapted to other countries or regions. The code (already including data sources from many other countries), as well as the figures are all available on github (***?***).

2 Background

2.1 Central epidemiological parameters of Covid-19 outbreak in Germany show that time-evolution is controlled by the effective growth rate

The initial phase of an epidemic outbreak, before any mitigation measures are taken, can typically be described by an SIR model with a constant spreading rate λ. Effects of mitigation measures leading to change points in λ (that we treat later) only manifest after starting mitigation measures and an observation delay, thus after about 16th of March in Germany. Because of the simplicity of this initial dynamics, we introduce the basic SIR model and its parameters using these data.

We estimate the central epidemiological parameters for our stationary SIR model (see Methods), specified by a spreading rate λ, a recovery rate μ, a reporting delay D, and the number of initially infected people I_0, with with Bayesian MCMC-sampling from the initial exponential phase of the epidemic outbreak in Germany (until 2020/03/15) (Fig. 1). We obtain as median estimates for the spreading rate $\lambda = 0.41$, $\mu = 0.12$, $D = 8.7$, and $I_0 = 18$. Overall, the model shows good agreement for both new infections C_t (Fig. 1 A) and the cumulative infections $\sum_{t'=0}^{t} C_{t'}$ (Fig. 1 B) with the expected exponential time dependence (linear in lin-log plot). The absolute deviation between data and model (Fig. 1 C) is well captured by the case-number-dependent width of our likelihood (Methods) motivated by demographic noise in mean-field models of spreading processes (*21, 22*). However, we observe that for some model parameters, the distribution of estimated parameters (the posterior distribution, Fig. 1 D-G histogram) is largely determined by our initial choice of assumed parameters (the prior distribution, Fig. 1 D-G blue line). In particular, only λ and I_0 are sufficiently constrained by the data, while μ an D are not.

[.] As long as the COVID-19 spread is still in the initial exponential onset phase, the SIR model can be approximated by an exponential growth (see Methods) with effective growth

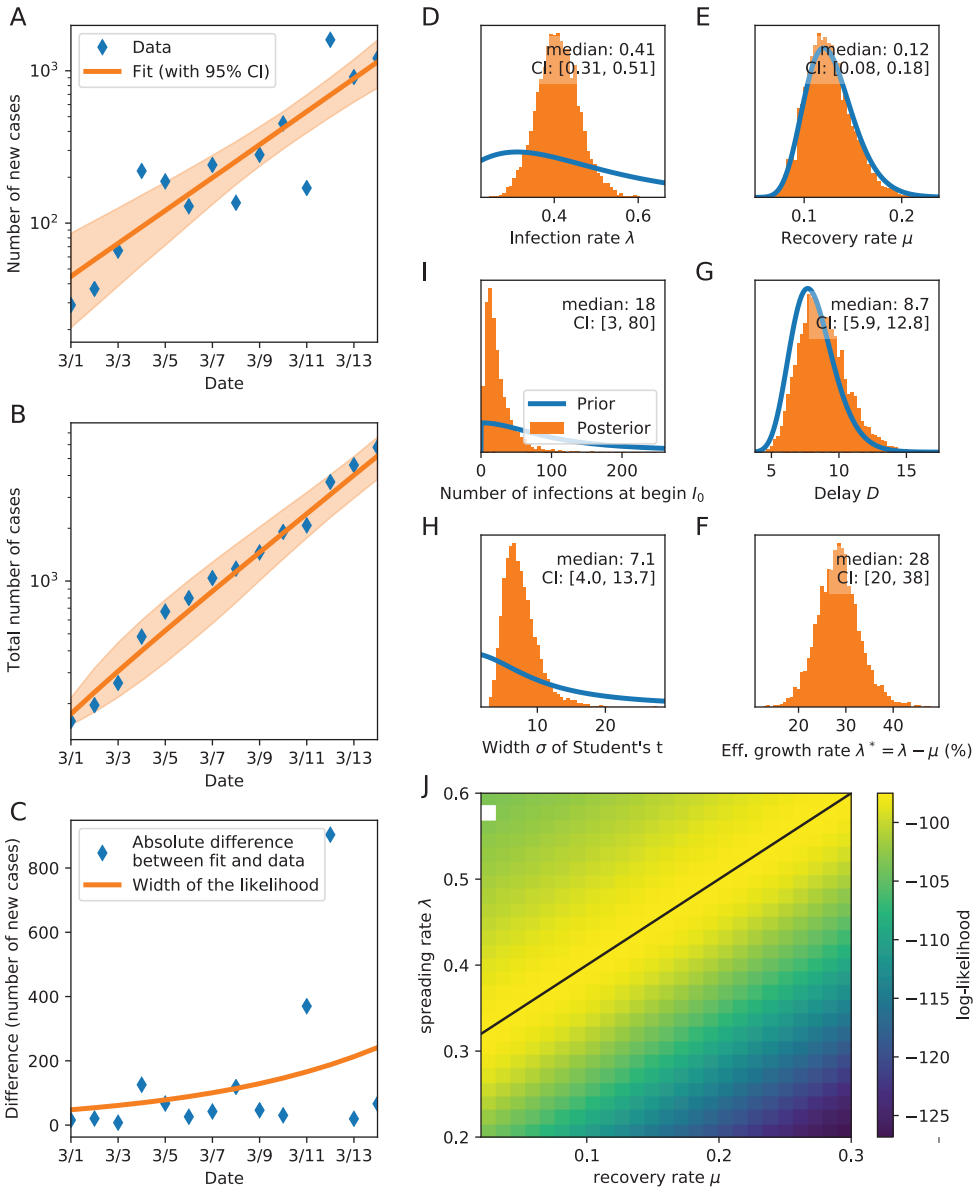

Figure 1: Parameters of the SIR model for the initial onset period (01-03-2020 until 15-03-2020) of the Covid-19 outbreak in Germany. **A:** Number of new cases over time. **B:** Same as A but for total number of cases over time (cumulative). C: Absolute difference between model and data (blue line) is well captured by the demographic-noise width we chose for the likelihood (Student's t-distribution). **D:** Estimated infection rate λ of the model, both estimated (orange) and prior (blue). **E:** Same as D for the recovery rate μ. **F:** Same as D for the effective growth rate $\lambda^* = \lambda - \mu$. **G:** Same as D for the delay D. **H:** Same as D for the width σ of the Student's t. The error of the likelihood function scales with the number of new cases as $\sigma\sqrt{C_t}$. **I:** Same as D for the initial number of cases I_0. **J:** Log-likelihood distribution for different combinations of λ and μ. A linear of λ and μ yield the same maximal likelihood (black line).

rate $\lambda^* = \lambda - \mu$ (Fig. 1). As a consequence, λ and μ cannot be estimated independently by the MCMC sampling in this early phase. This is further supported by a systematic scan of the model's log-likelihood in the λ–μ space showing an equipotential line for the maximum likelihood (Fig. 1 J). This verifies that the effective growth rate is the relevant free parameter with median $\lambda^* = 28\%$ from the complete MCMC sampling (Fig. 1 F).

[.] The control parameter of the dynamics in the exponential onset phase is thus the effective growth rate $\lambda^* = \lambda - \mu$ (Fig. 1 F): if the infection rate is larger than the recovery rate ($\lambda > \mu$), case numbers grow exponentially; with ($\lambda < \mu$) the recovery dominates, and the spread is diminished; the unstable and stable dynamics are separated by a critical point with $\lambda = \mu$ (*22*). Expressed in terms of reproductive number, $R = 1$ separates the unstable from the stable regime. If translated into a basic reproduction number R_0, our estimates during the initial onset phase yield a median value $R_0 = \lambda/\mu = 3.13 > 1$, consistent with previous reports that find values between 2.3 and 3.3 (*19, 23, 24*). The aim of any policy that diminishes the spread is thus to lower the infection rate and increase the recovery rate, such that on expectation one person infects less than one person ($R < 1$).

3 Timing of interventions matters for the mitigation of the outbreak

One ulterior motivation for the parameter estimation from past disease spread is to forecast future case numbers, and how they are impacted by political interventions. By modeling different interventions, we show that both, the amount of change in behavior (leading to a change in spreading rate λ, Fig. 2 A,B) and the exact timing of the change (Fig. 2 C,D) determine the future development.

After parameter distributions were inferred on the real-world data up until 2020/03/15, the interventions were implemented by adapting the past (inferred) spreading rate λ_0 to a new value

λ_1 that reflects the change in public behaviour: **(I) No social distancing;** Public behaviour is unaltered and the spread continues with the inferred rate ($\lambda_1 = \lambda_0$). **(II) Mild social distancing;** The spreading rate decreases to 50%, ($\lambda_1 = \lambda_0 \,/\, 2$). Although people cut the average number of contacts they meet in half, the exponential increase in the total number of reported cases continues for another 8 days, before any effect is visible. This duration matches the reporting delay between exposure (transmission of the virus to a new susceptible person) and the reporting of the case. **(III) Strong social distancing;** The spreading rate decreases to 10%, ($\lambda_1 = \lambda_0 \,/\, 10$). Contacts are severely limited, but even when people stay at home as much as possible, *some* contacts are unavoidable. Even under such drastic policy changes, no effect is visible until the reporting delay is over. Thereafter, a quick decrease in daily new infections manifests within two weeks and the total number of cases reaches a stable plateau. In this scenario, a plateau is reached because the new infection rate $\lambda_1 \approx 0.04$ is smaller than the recovery rate $\mu = 0.125$.

[.] Timing matters: Apart from the strength of an intervention, its *onset* time has great impact on the total case number (Fig. 2 C,D). For example, focusing on intervention (III) — where a stable plateau is reached — the effect of advancing or delaying the change $\lambda_0 \to \lambda_1$ by just five days leads to more than a 3-fold difference in cumulative cases. While we find that this onset of an intervention has great effect on case numbers, the duration over which the change takes place has only minor effect. In Fig. 2 E,F we illustrate the adjustment of $\lambda_0 \to \lambda_1$ for durations of 14, 7 and 1 day(s). Note that the duration of the adjustment is a simple choice to incorporate variability in individual behaviour, and is not linked to the reporting delay D.

4 Change point detection reveals the effect of two past interventions on the outbreak of COVID-19 in Germany

[.] As long as a disease spreads basically unnoticed by the community, the model parameters can be considered stationary (fixed). However, the COVID-19 spread in Germany has by mid-

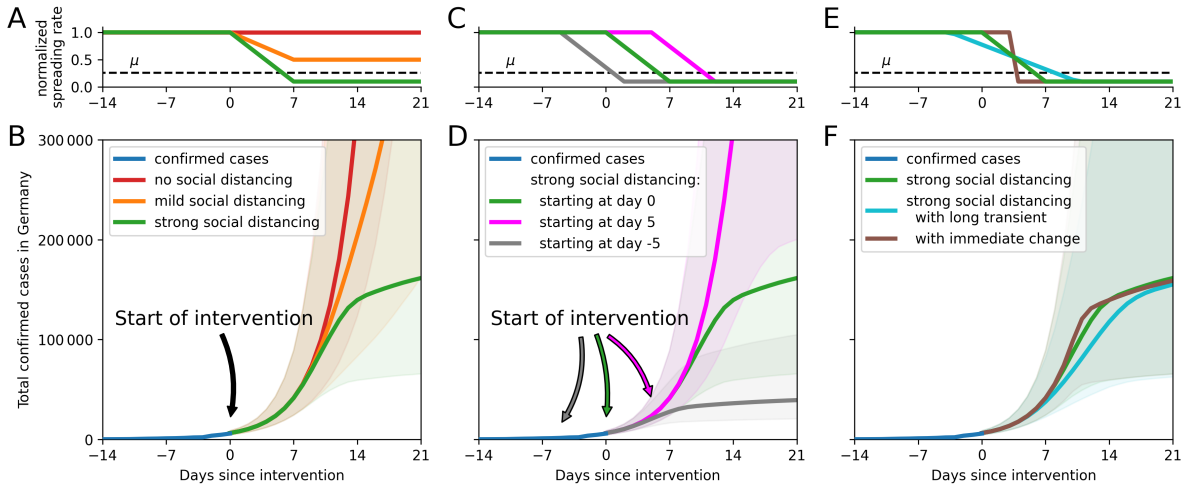

Figure 2: Timing and effectiveness of interventions shape case numbers.**A, B:** Three differently strong interventions create scenarios for the development of confirmed COVID-19 cases in Germany up to 2020/03/15: (I) no social distancing — red, (II) mild social distancing — orange, or (III) strict social distancing — green. **C, D:** We also analyzed how a delayed restriction impacts case numbers: Strict restrictions starting on 2020/03/15 (green), or five days later (magenta). A delay of five days in implementing restrictions has a major impact on the expected case numbers. Starting the same intervention five days earlier (later) decreases (increases) the total number of cases roughly by a factor three. **E, F:** Comparison of the time over which interventions ramp up to full effect.

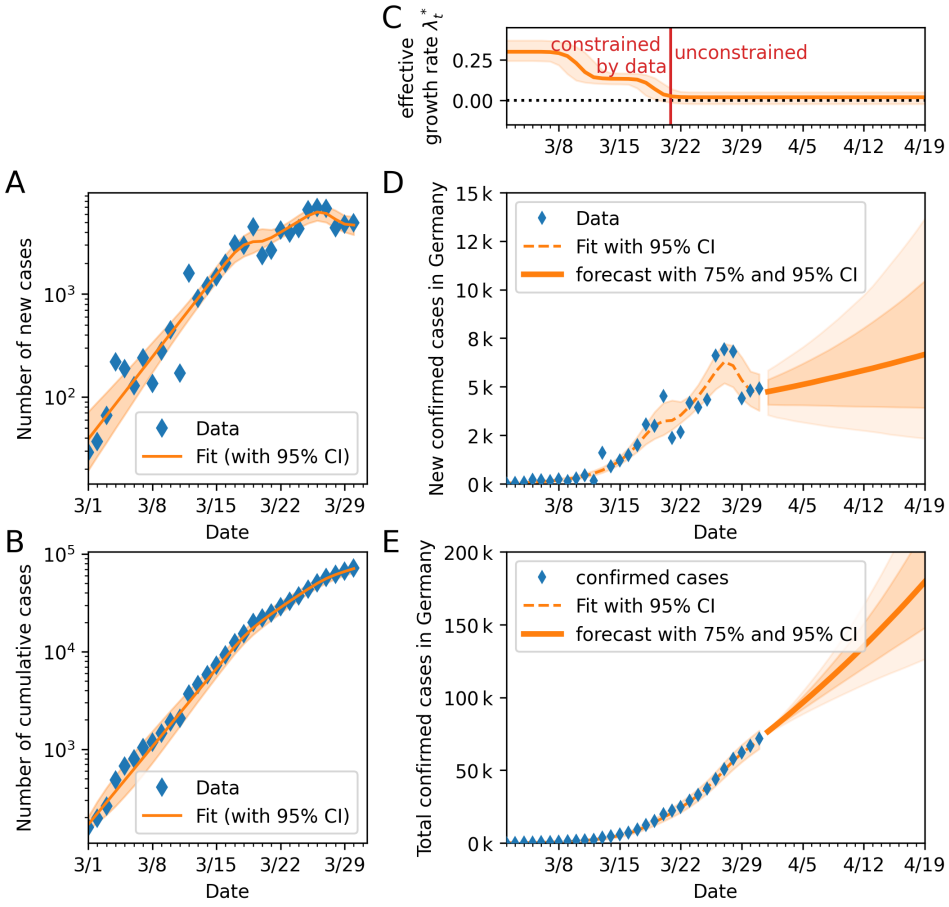

Figure 3: Inferring (the time of) the changing point in spreading rate λ. **A:** Comparison of daily recorded new cases and the model, log scale. **B:** Comparison of total recorded cases and the model, log scale. **C:** Time-dependent model-estimate of the spreading rate λ_t. **D:** Model forecast of new cases, based on the inferred λ_t, linear scale. **E:** Model forecast of total cases, based on the inferred λ_t, linear scale.

March led to a considerable change in policy and in the behavior of individuals, starting from washing hands more thoroughly and stricter self-isolation upon suspicious symptoms to formal measures like closing public events and places, schools and even a "Kontaktsperre". The aim of all these measures is to reduce the effective spreading rate λ and increase μ. As soon as the recovery rate μ is larger than λ, the number of new confirmed infections should diminish (after the respective delay). A central challenge is to detect the change points in the spread λ and quantify the amount of change. Ideally, this change can then be related to the change in behavior, so that one gains an understanding about the effectiveness of the different measures.

To detect potential changes in λ, we assumed (for now) up to three potential changes in λ, thus λ switching from λ_0 (initial spread during the exponential growth phase) to λ_1, λ_2 and λ_3 (Fig. 4 A,B). We expect each change to unfold over a few days (Fig. 4 G,H). The first change point is expected to result from the official changes in policies around March 8th where large gatherings like soccer matches and fairs were banned. A second change point is expected around March 15th, where schools and many shops were closed. A third change point is expected around March 22nd, where all non essential shops were closed, and a "Kontaktsperre" was enacted. As described above the behavioral changes introduced at these change points take a certain time to show an effect in the observed data.

Formal, LOO-based model comparison indicated that the models with 2 and 3 change points describe the data better than the models with 0 or 1 change point. The model with 2 change points nominally was the best model, yet the difference between the two best models was considerably smaller than the standard errors of the LOO-score estimates, and is thus not reliably interpretable. Based on the known timing of the third intervention, and our estimates for the delay D (posterior median, 9.5 days), however, we still favor the model with two change points for a description of the current situation.The model with none or a single change point, however, have a LOO-score that are at least about 1 standard deviation lower than than those of the two

Table 1: Model comparison.

Scenario	LOO-score	pLOO
zero change points	491(16)	4.80
one change point	469(17)	10.67
two change points	449(16)	7.85
three change points	449(16)	8.00

best models and can be discounted.

With the inclusion of these potential change points into our family of models, we found indeed evidence for two change points: First, λ decreased from $\lambda_0 = 0.41$ (CI [0.34 0.49]) to $\lambda_1 = 0.25$ (CI [0.2 0.3]). Effectively, the growth rate $\lambda^* = \lambda - \mu$ decreased by more than a factor 2, from 0.29 to 0.13. The date of the change point is inferred to be the 7th/8th of March (95% CI [4th to 11th])], hence matching very well the timing of the first political actions like cancelling soccer games, as well as increased awareness, which certainly changed the behavior of individuals.

Second, as of beginning of April, the data start to be informative about the second change point from λ_1 to λ_2 as well. However, there is still hardly any difference between prior and posterior distributions for λ_2, t_2. Our prior assumption is that the reduction from λ_1 to λ_2 follows a similar factor of 2 as the first change from λ_0 to λ_1, and that the change point is located around around March 15th (see above).

Because we have clear evidence for a first change point, matching the first political intervention, and we start to also have evidence for a second one, matching the second intervention, we here consider the potential future action of a third change point a week later as well.

Overall, λ_0 inferred from the model with change points is very similar to λ inferred above from the simpler model, which assumed a stationary λ and was fitted only with data until March 16th (Fig. 1 A). As before, the data provide little information on μ (Fig. 4 D). The relevant parameter is the effective growth rate $\lambda^* = \lambda - \mu$. The $\lambda^* > 0$ (or $\lambda^* < 0$) determines the

exponential growth (or decay) rate.

[.]The durations over which the changes are taking place (transients t_1 and t_2) are not expected to have a major impact on the results (see Fig. 2 E,F, scenarios). Also the scale factor σ and the number of initial infections I_0 are completely consistent with the initial model inference during the exponential onset phase above (cf Fig. 1).

[.]When comparing our inference based on the time-varying λ and its change-points to the number of confirmed cases, we find a clear match (Fig. 7 A,B). Note that the tell-tale kink in the data is more evident in the raw number of newly confirmed cases (Fig. 7 A) than in the cumulative report (Fig. 7 B). The inferred temporal decrease of new cases before increasing again comes from changing an exponential growth rate over small interval in the model. It is consistent with the observed temporary drop newly confirmed cases and suggests a rapid implementation of mitigation measures by the public.

We also observed spread in the data points that was somewhat larger than expected by the model. We assign this to the fact that we did not incorporate an additional prior describing on the uncertainty and noise that is introduced by fluctuations in reporting (less reports on weekends, availability of test kits, etc.). Given this caveat, we consider the match of model and data convincing.

Whereas the data provide sufficient information about the first change-point (Fig. 4 A,B,E), the second and third ones are not well constrained yet (Fig. 4 C,F, SI Figs. [corresponding SI for one and 3 change points]). Therefore, we show the results for all, the model with one, two and three change points in the main figure (Fig. 0, [on github/1 page summary]). Displaying all three scenarios enables one to compare forecasts with zero, two or three change points (Fig. 0). It becomes clear that in the current phase, where we know about the presence of two further change points, but know very little about their effect, the future development of case numbers displays a large range of uncertainty. Nonetheless, we expect that the second change point

brought the disease spread close to the critical transition, which separates exponential growth of new cases from a decline, thus a unstable system to a stable one. Together with a third potential change point, this leaves us with some optimism that the disease spread can be brought under control if the social distancing measures remain to be sufficiently strong.

5 Discussion

We here presented a SIR model with a potential change points for spreading rate combined with Bayesian parameter estimation. This model allowed us to estimate the unperturbed central basic epidemiological parameters in the earliest days of the COVID19 outbreak in Germany, but also the detection of two change points in the spreading rate. We could show that change points in the spreading rate will be reflected in confirmed case numbers with a median delay of $D = 9.5$ days and could, this way, link the observed changes to two measures taken by the German government: (1) travel warnings, and the ban on all large events with more than 1000 participants, effected on March 8th and (2) the closing of schools and childcare centers by March 17th.

The introduction of explicit modeling of change points has a considerable advantage in terms of data efficiency in that all available data could be used for estimating change-point independent model parameters. As long as it is plausible that additional measures will not change model parameters other than λ our approach can be extend by adding further change points and then be reused for further short-term forecasts. Under novel developments, such as the introduction of novel, effective therapies influencing the recovery rate μ our approach provides the algorithmic blueprint for modeling and detecting such change points as well.

Importantly, our approach also avoids problems encountered in forecasting newly confirmed case numbers when naively combining an updated assumption of the spreading rate with the current pool of confirmed cases (i.e. ignoring the delay D). For example, such a naive combi-

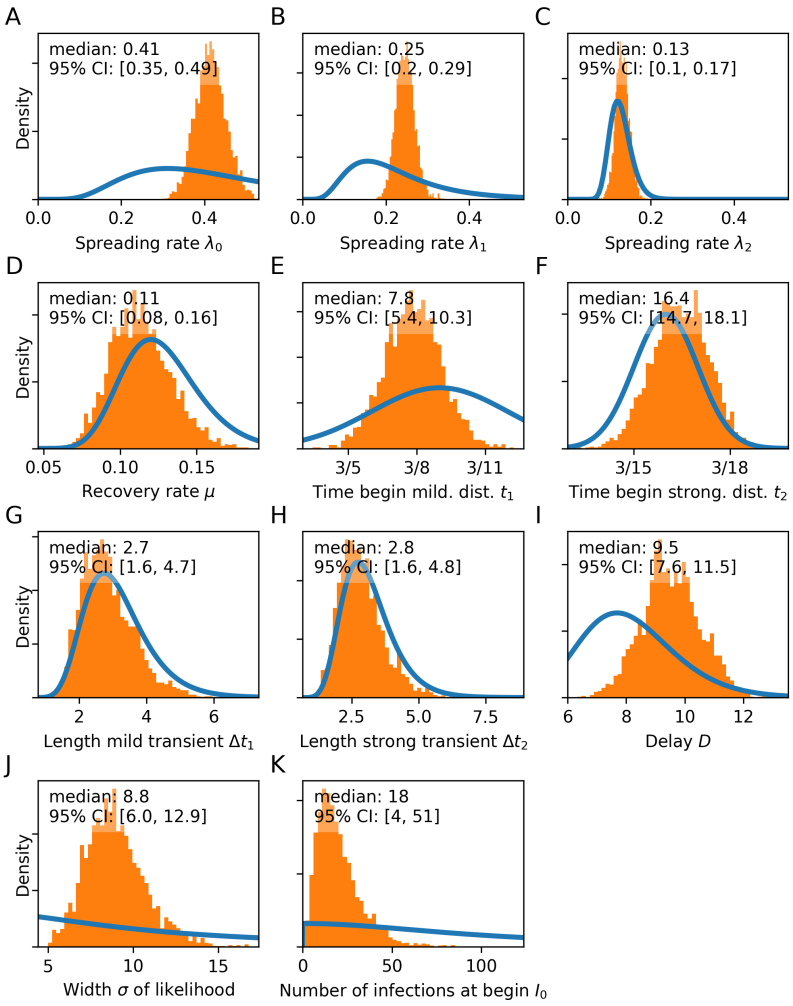

Figure 4: Posterior distributions from the change-point detection with 2 change points compared to prior distributions.

nation would unable to explain the temporary drop followed by another rise that is observed in the newly reported cases around the time that a change in λ starts to be visible in the data (see Fig. 7).

Our model comparison also ruled out models without a change point or with only one change point. While this may seem trivial, it has important consequences for making the short term forecasts that decision makers in society rely on, e.g. to provision resources. These important consequences are linked to the dynamics of exponential growth of case numbers, where even minor changes in the spreading rates lead to large differences in forecasts within just a few days. Hence, it is important to look out for and identify potential change points as early as possible, as is possible using our model.

Our results rely on a fairly simple implementation of time-varying spreading rates, as assumed the spreading rates to be constant in time, except for rate changes occurring only at the time of interventions – the change points – where we formulated broad prior distributions for the new spreading rate and the time of the change. Our result seem to indicate that this modeling approach is sufficient at present: While we introduced fairly broad priors on the spreading rates we obtained a fairly narrow posterior distribution for the changed spreading rates (Fig. 6B), indicating that the assumption of discrete steps in the spreading rates is viable. With respect to the posterior distributions for the dates of the change points, we also found the data to provide valuable information in narrowing the posterior distribution for the first change point, compared to the prior, and in slightly moving the posterior mode for the second change point.

Change point detection and interpretation hinges on proper estimation on the delay D between a new infection and recording a newly confirmed case. Thus, it seems important to assess whether the posterior median value of $D = 9.5$ days is at least compatible with what is known. In our model D sums up at least three separate factors, i.e. the biological incubation period, and an additional delay from first very mild symptoms to symptoms warranting testing under the

constraint of limiting testing capacities, and a possible delay before a testing slot is available. At present, the incubation is reported by the WHO as being in a broad range from 1-14 days with a mean of 5 days [REF], and the WHO states that 'symptoms are usually mild and begin gradually'. A gradual onset of symptoms may delay testing because people tend to wait before asking for being tested, or will be asked to wait as testing in more urgent cases is prioritized. Adding a mean of 5 days of incubation period to the patient waiting for three days after gradual symptom onset before asking for a test, and waiting 1 days for a test would be a plausible scenario in Germany. The resulting 9 days are compatible with the median and spread of the posterior of D we found here, given the wide range of durations for the incubation period. The posterior median of $D = 9.5$ days in our model. It should be noted in addition, that once mass-testing for asymptomatic members of the general population is available, or even mandatory, a change point for D will certainly have to be added to the model.

Since most of the forecast uncertainty comes from scenario assumptions and uncertainties in model parameters, we purposely kept the dynamic model as simple as possible for it to remain tractable. Focusing on a simple model, we have excluded many details that are relevant for precise modelling of epidemics, especially at very late stages or in small populations. Such details include explicit (modeling of) incubation times (***?**, 25*), spatial heterogeneity (*?, 15*), isolation (*14, 25*), or subsampling effects hiding undetected cases even beyond the reporting delay (*26*). However, we argue that most of these effects are small compared to the scale of uncertainty between different forecast scenarios that may help decision makers take action, and for short term forecasts.

In conclusion, we argue that any forecast needs to be accompanied with a detailed discussion of the underlying assumptions. Our Bayesian approach forced us to formulate all assumptions (prior distributions and scenarios). The assumptions should include as much information as possible and they should be communicated alongside with the forecast. Only a forecast along with

the underlying assumptions form a basis to advise decision makers to make a choice between different future interventions. Of course, this requires to formulate a set of plausible scenarios in terms of a target outcome (in our case to reduce the spreading rate to 50% or 10%). It is then not a forecast what happens for a particular intervention, but a forecast what is likely to happen in case the intervention has the desired effect. Any intervention should then be evaluated within the Bayesian framework in order to judge the anticipated effect. However, such a live validation requires patience for the interventions to become effective — which can take as long as 2 weeks as we have shown for the case of COVID-19.

6 Materials and methods

As a basis for our forecast scenarios, we use the differential equations of the well-established SIR (Susceptible-Infected-Recovered) model. While the model dynamics are well understood in general, here our main challenge is to estimate model parameters specifically for the COVID-19 outbreak. To that end, we combined a Bayesian approach — to incorporate prior knowledge — with Markov Chain Monte Carlo (MCMC) sampling — to explore the parameters. Put simply, we first estimate the parameter distribution that best describes the observed situation, and then we use many samples from this parameter distribution to evolve the model equations and thus forecast future developments.

6.1 Simple model: SIR model with stationary spreading rate λ

We consider a time-discrete version of the standard SIR model. In short, we assume that the disease spreads at rate λ from the infected population stock (I) to the susceptible population stock (S), and that the infected stock recovers (R) at rate μ. This well-established model for disease spreading can be described by the following set of (deterministic) ordinary differential

equations (see, e.g., Refs (*3, 4, 14*)). Within a population of size N,

$$\begin{aligned} \frac{\mathrm{d}S}{\mathrm{d}t} &= -\lambda \frac{SI}{N} \\ \frac{\mathrm{d}I}{\mathrm{d}t} &= \lambda \frac{SI}{N} - \mu I \\ \frac{\mathrm{d}R}{\mathrm{d}t} &= \mu I \,. \end{aligned} \tag{1}$$

As a remark, during the onset phase of an epidemic only a very small fraction of the population is infected (I) or recovered (R), and thus $S \approx N \gg I$ such that $S/N \approx 1$. Therefore, the differential equation for the infected reduces to a simple linear equation, exhibiting an exponential growth

$$\frac{dI}{dt} = (\lambda - \mu) I \quad \text{solved by} \quad \mathrm{I(t) = I(0)\, e^{(\lambda-\mu)t}} \,. \tag{2}$$

Because our data set is discrete in time (Δt =1 day), we solve the above differential equations with a discrete time step ($\mathrm{d}I/\mathrm{d}t \approx \Delta I/\Delta t$), such that

$$\begin{aligned} S_t - S_{t-1} &= -\lambda \Delta t \tfrac{S_{t-1}}{N} I_{t-1} &&=: -I_t^{\mathrm{new}} \\ R_t - R_{t-1} &= \mu \Delta t I_{t-1} &&=: \quad R_t^{\mathrm{new}} \\ I_t - I_{t-1} &= \left(\lambda \tfrac{S_{t-1}}{N} - \mu\right) \Delta t I_{t-1} = I_t^{\mathrm{new}} - R_t^{\mathrm{new}} \,. \end{aligned} \tag{3}$$

Importantly, I_t models the number of all (currently) active infected people, while I_t^{new} is the number of new infections that will eventually be reported according to standard WHO convention. Importantly, we explicitly include a reporting delay D between new infections I_t^{new} and newly reported cases (C_t) as

$$C_t = I_{t-D}^{\mathrm{new}}. \tag{4}$$

We begin our simulations at time $t = 0$ with I_0 infected cases and start including real-word data of reported cases $\hat{C}_t$ from day $t > D$ (see below for a parameterization).

Full model: SIR model with change points in λ

Our change-point detection builds on a generalization of the simple SIR model with stationary spreading rate. Instead, we now assume that the spreading rate λ_i, $i = 1, ..., n$, may change

at certain time points t_i from λ_{i-1} to λ_i, linearly over a time window of Δt_i days. Thereby, we account for policy changes to reduce λ, which were implemented in Germany step-by-step. Thus, the parameters t_i, Δt_i, and λ_i are added to the parameter set of the simple model above, and the differential equations are augmented by the time-varying λ_i.

Estimating model parameters with Bayesian MCMC

We estimate the set of model parameters $\theta = \{\lambda_i, t_i, \mu, D, \sigma, I_0\}$ using Bayesian inference with Markov-chain Monte-Carlo (MCMC). The parameter σ is the scale factor for the width of the likelihood $P\left(\hat{C}_t|\theta\right)$ between observed data and model (see below). Our implementation relies on the python package pymc3 (*27*) with NUTS (No-U-Turn Sampling) (*28*). The structure of our approach is the following:

Choose random initial parameters and evolve according to model equations. Initially, we choose parameters θ from prior distributions that we explicitly specify below. Then, time integration of the model equations generates a (fully deterministic) time series of new infected cases $C(\theta) = \{C_t(\theta)\}$ of the same length as the observed real-world data $\hat{C} = \left\{\hat{C}_t\right\}$.

Iteratively update the parameters using MCMC. The drawing of new candidate parameters and the time integration of the SIR model is repeated in every MCMC step. The idea is to probabilistically draw parameter updates and to accept them such that the deviation between the model outcome and the available real-world time-series is likely to reduce. We quantify the deviation between the model outcome for one time point t, $C_t(\theta)$ and the corresponding real-world data point $\hat{C}_t$ with the local likelihood

$$p\left(\hat{C}_t|\theta\right) \sim \mathrm{StudentT}_{\nu=4}\left(\mathrm{mean} = \mathrm{C_t}(\theta),\ \mathrm{width} = \sigma\sqrt{\mathrm{C_t}(\theta)}\right) .$$

We chose the Student's t-distribution because it resembles a Gaussian distribution around the mean but features heavy tails, which make the MCMC more robust with respect to outliers (*29*). The case-number-dependent width models the demographic noise of typical mean-field solutions for epidemic spreading, e.g., $\dot{\rho}(t) = a\rho(t) - b\rho^2(t) + \sqrt{\rho(t)}\eta(t)$, where ρ is the activity and $\eta(t)$ is Gaussian white noise (*21, 22*). This choice is consistent with our data (Fig. 1 A-C). The overall deviation is then simply the product of local likelihoods over all time points.

For each MCMC step, the new parameters are drawn so that a set of parameters that minimizes the previous deviation is more likely to be chosen. In our case, this is done with an advanced gradient-based method (NUTS (*28*)). To reiterate, every time integration that is performed has its own set of parameters and yields one complete model time series. If the time integration describes the data well the parameter set is accepted, and this yields one Monte Carlo sample of the model parameters for the posterior distribution; the MCMC step is then repeated to create more samples from the posterior. Eventually, the majority of accepted parameter samples will describe the real-world data well, so that consistent forecasts are possible in the forecast phase.

Forecast using Monte Carlo samples. For the forecast, we take all samples from the MCMC step and continue time integration according to different forecast scenarios explained below. Note that the overall procedure yields an ensemble of forecasts — as opposed to a single forecast that would be solely based on one set of (previously optimized) parameters.

Priors that constrain model parameters

As forecasts are needed rapidly at the onset of an epidemic, the available real-world data is typically not informative enough to identify all free parameters, or to empirically find their underlying distributions. We therefore chose informative priors on initial model parameters

Table 2: Priors on the model parameters for the SIR model with stationary spreading rate.

Parameter	Prior distribution
spreading rate λ	$\mathrm{LogNormal}(\log(0.4), 0.5)$
recovery rate μ	$\mathrm{LogNormal}(\log(1/8), 0.2)$
reporting delay D	$\mathrm{LogNormal}(\log(8), 0.2)$
initially infected I_0	$\mathrm{HalfCauchy}(100)$
scale factor σ	$\mathrm{HalfCauchy}(10)$

where possible and complemented with uninformative priors else. Our choices are summarized in Tab. 2 for the simple model, SIR model with stationary spreading rate for the exponential onset phase, and in Tab. 3 for the full model with change points, and justified in the following.

Priors for the simple model (Tab. 2): In order to constrain our simple model, an SIR model with stationary spreading rate for the exponential onset phase, we chose the following informative priors. Because of the ambiguity between the spreading and recovery rate in the exponential onset phase (see Simple model), we chose a narrow log-normal prior for the recovery rate $\mu \sim \mathrm{LogNormal}(\log(1/8), 0.2)$ with median recovery time of 8 days (*14*) (including both actual recovery as well as any isolation measures taken, in principle difficult to estimate) but a broad log-normal prior distribution for the spreading rate $\lambda \sim \mathrm{LogNormal}(\log(0.4), 0.5)$ with median 0.4. This way, the prior for $-\mu$ has median 0.275 and the prior for the base reproduction number(λ/μ) has median 3.2 consistent with the broad range of previous estimates (*19, 23, 24*). In addition, we chose a log-normal prior for the reporting delay $D \sim \mathrm{LogNormal}(\log(8), 0.2)$ to incorporate both the incubation time between 1–14 days with median 5 (***?**, 30*) plus a delay from infected people waiting to contact the doctor and get tested.

The remaining model parameters are constrained by uninformative priors, in practice the Half-Cauchy distribution (*31*). The half-Cauchy distribution $\mathrm{HalfCauchy}(\mathrm{x}, \beta) = 2/\pi\beta[1 + (\mathrm{x}/\beta)^2]$ is essentially a flat prior from zero to $O(\beta)$ with heavy tails beyond. Therby, β merely sets the order of magnitude that should not be exceeded for a given parameter. We chose for

Table 3: Priors on the model parameters for the SIR model with change points.

Parameter	Prior distribution
change points t_1	$\mathrm{Normal}(2020/03/09, 3)$
t_2	$\mathrm{Normal}(2020/03/15, 1)$
t_3	$\mathrm{Normal}(2020/03/22, 1)$
change duration Δt_i	$\mathrm{LogNormal}(\log(3), 0.3)$
spreading rates λ_0	$\mathrm{LogNormal}(\log(0.4), 0.5)$
λ_1	$\mathrm{LogNormal}(\log(0.2), 0.5)$
λ_2	$\mathrm{LogNormal}(\log(1/8), 0.2)$
λ_3	$\mathrm{LogNormal}(\log(1/16), 0.2)$
recovery rate μ	$\mathrm{LogNormal}(\log(1/8), 0.2)$
reporting delay D	$\mathrm{LogNormal}(\log(8), 0.2)$
initially infected I_0	$\mathrm{HalfCauchy}(100)$
scale factor σ	$\mathrm{HalfCauchy}(10)$

the number of initially infected people in the model (16 days before first data point) $I_0 \sim \mathrm{HalfCauchy}(100)$ assuming an order of magnitude $O(100)$ and below. In addition, we chose of the scale factor of the width of the likelihood function $\sigma \sim \mathrm{HalfCauchy}(10)$, which is further multiplied to the number of new cases.

Priors for the full model (Tab. 3): In order to constrain our full model, an SIR model with change points in the spreading rate, we chose the same priors as for the simple model but added the required priors associated with the change points.

For the timing of change points, we chose normal distributed priors. In particular, we chose for the first change point $t_1 \sim \mathrm{Normal}(2020/03/09, 3)$ because on n the weekend of March 8, large public events like visits to soccer matches or fairs were cancelled. We chose for the second change point $t_2 \sim \mathrm{Normal}(2020/03/15, 1)$, because on March 15, the closing of schools and other educational institutions along with the closing of non-essential stores were announced and implemented on the following day. Restaurants were allowed to stay open until 6 pm. We chose for the third change point $t_3 \sim \mathrm{Normal}(2020/03/22, 1)$, because on March 22, a far-reaching contact ban ("Kontaktsperre"), which includes the prohibition of even small public

gatherings as well as complete closing of restaurants and non-essential shops was imposed by the government authorities. Further policy changes may occur in future; however, for now, we do not include more change points. We model the time dependence of λ as change points, and not as continuous changes, because the policy changes were incurred in these three discrete steps, and in our observations were adhered by the public. Continuous changes, originating e.g. from increased awareness of the population can be accounted for by the discrete steps as well, within the precision of reported cases we have.

The change points take effect over a certain time period Δt_i for which we choose $\Delta t_i \sim \mathrm{LogNormal}(\log(3), 0.3)$ with a median of 3 days over which the spreading rate changes continuously as interventions have to become effective. The precise duration of the transition has hardly any affect on the cumulative number of cases (Fig. 2 E-F). We assumed a duration of three days, because some policies were not announced at the same day for all states within Germany; moreover, the smooth transition also can absorb continuous changes in behavior.

For the spreading rates, we chose log-normal distributed priors as in the simple model. In particular, we chose for the initial spreading rate the same prior as in the simple model, $\lambda_0 \sim \mathrm{LogNormal}(\log(0.4), 0.5)$; for the first change point $\lambda_1 \sim \mathrm{LogNormal}(\log(0.2), 0.5)$, assuming the first intervention to reduce the spreading rate by 50% from our initial estimates ($\lambda_0 \approx 0.4$) with a broad prior distribution; for the second change point $\lambda_2 \sim \mathrm{LogNormal}(\log(1/8), 0.2)$, assuming the second intervention to reduce the spreading rate to the level of the recovery rate, which would lead to a stationary number of new infections. This corresponds approximately to a reduction of λ at the change point by 50%; and for the third change point $\lambda_3 \sim \mathrm{LogNormal}(\log(1/16), 0.2)$, assuming the third intervention to reduce the spreading rate again by 50%. With that intervention, λ_3 is smaller than the recovery rate μ, causing a decrease in new case numbers and a saturation of the cumulative number of infections. In general, we assume that each package of governmental interventions (together with the increasing awareness)

leads to a reduction (and not an increase) of λ at a change point. As we cannot know yet the precise reduction factor, we adhere to assume a reduction by 50%, but always with a fairly wide uncertainty, so that in principle even an increase at the change point would be possible.

Using change points has the advantage that extrapolation to future behavior assumes no further change in λ apart from the change points. That facilitates the understanding of future scenarios. In a future iteration of the model, we will compare continuous versus change-point behavior.

Model comparison

Since change point detection entails evaluating models with different numbers of parameters, some form of fair model comparison needs to be performed. Here, we compared the models with different numbers of change points by their pointwise out-of-sample prediction accuracy using the log-likelihood evaluated at the posterior simulations of the parameter values obtained from the fitted models. Out-of-sample accuracy was approximated using Leave-one-out cross-validation (LOO) [Ref Gelman 2016].

References

1. M. Enserink, K. Kupferschmidt, *Science* **367**, 1414 (2020).
2. W. O. Kermack, A. G. McKendrick, G. T. Walker, *Proceedings of the Royal Society of London. Series A, Containing Papers of a Mathematical and Physical Character* **115**, 700 (1927).
3. H. Hethcote, *SIAM Rev.* **42**, 599 (2000).
4. J. Anderson, I. Lampl, I. Reichova, M. Carandini, D. Ferster, *Nat. Neurosci.* **3**, 617 (2000).
5. N. C. Grassly, C. Fraser, *Nat Rev Microbiol* **6**, 477 (2008).

Table 4: Overview of model parameters.

Variable	Parameter
$\theta = \{\lambda_i, t_i, \mu, \sigma, I_0\}$	Set of model parameters that are optimized
λ	Spreading rate
μ	Recovery rate
$\lambda^* = \lambda - \mu$	Effective spreading rate
λ_i	Spreading rate after i-th intervention
t_i	time of i-th intervention
σ	Scale factor of the width of Student's t-distribution
N	Population size (83.700.000)
S_t	Susceptible at time t
I_t	Infected at time t
R_t	Recovered at time t
Δt	Time step
$R_t^{\text{new}} = \mu \Delta t I_{t-1}$	New recoveries at time t
$I_t^{\text{new}} = \lambda \Delta t \frac{S_{t-1}}{N} I_{t-1}$	New infections at time t
$C_t = I_{t-D}^{\text{new}}$	New reported cases at time t
D	Delay of case detection
$p\left(\theta \middle\vert \hat{C}_t\right)$	Posterior distribution with respect to the observed data

6. R. Parshani, S. Carmi, S. Havlin, *Phys. Rev. Lett.* **104**, 258701 (2010).

7. T. Harko, F. S. N. Lobo, M. K. Mak, *Applied Mathematics and Computation* **236**, 184 (2014).

8. B. Shulgin, L. Stone, Z. Agur, *Bull. Math. Biol.* **60**, 1123 (1998).

9. O. N. Bjørnstad, B. F. Finkenstädt, B. T. Grenfell, *Ecol. Monogr.* **72**, 169 (2002).

10. L. Hufnagel, D. Brockmann, T. Geisel, *Proc. Natl. Acad. Sci. USA* **101**, 15124 (2004).

11. T. Britton, P. D. O'Neill, *Scand J Stat* **29**, 375 (2002).

12. J. Lourenço, *et al.*, *eLife* **6**, e29820 (2017).

13. N. R. Faria, *et al.*, *Sci Rep* **7**, 1 (2017).

14. B. F. Maier, D. Brockmann, *ArXiv200207572 Phys. Q-Bio* (2020).

15. P. Bittihn, R. Golestanian, *ArXiv200308784 Phys. Q-Bio* (2020).

16. R. M. Anderson, H. Heesterbeek, D. Klinkenberg, T. D. Hollingsworth, *The Lancet* **395**, 931 (2020).

17. J. R. Fauver, *et al.*, *medRxiv* p. 2020.03.25.20043828 (2020).

18. R. Li, *et al.*, *Science* (2020).

19. A. J. Kucharski, *et al.*, *The Lancet Infectious Diseases* (2020).

20. J. Lourenco, *et al.*, *medRxiv* p. 2020.03.24.20042291 (2020).

21. S. di Santo, P. Villegas, R. Burioni, M. A. Muñoz, *Phys. Rev. E* **95** (2017).

22. M. A. Muñoz, *Rev. Mod. Phys.* **90**, 031001 (2018).

23. J. Zhang, *et al.*, Age profile of susceptibility, mixing, and social distancing shape the dynamics of the novel coronavirus disease 2019 outbreak in China, *Preprint*, Epidemiology (2020).

24. Y. Liu, A. A. Gayle, A. Wilder-Smith, J. Rocklöv, *J Travel Med* **27** (2020).

25. L. Peng, W. Yang, D. Zhang, C. Zhuge, L. Hong, *ArXiv200206563 Q-Bio* (2020).

26. J. Wilting, V. Priesemann, *Nat. Commun.* **9**, 2325 (2018).

27. J. Salvatier, T. V. Wiecki, C. Fonnesbeck, *PeerJ Comput. Sci.* **2**, e55 (2016).

28. M. D. Hoffman, A. Gelman, *J. Mach. Learn. Res.* **15**, 1593 (2014).

29. K. L. Lange, R. J. A. Little, J. M. G. Taylor, *J. Am. Stat. Assoc.* **84**, 881 (1989).

30. S. A. Lauer, *et al.*, *Ann Intern Med* (2020).

31. A. Gelman, *Bayesian Anal.* **1**, 515 (2006).

Acknowledgments

We thank Tim Friede, Theo Geisel and Vladimir Zykov for carefully and promptly reviewing our work internally. We thank the Priesemann group - especially Matthias Loidolt, Daniel Gonzalez Marx, Fabian Mikulasch, Lucas Rudelt & Andreas Schneider - for exciting discussions and for their valuable comments. We thank the colleagues of the Göttingen Campus, with whom we were discussing the project and the case forecast in the past weeks very intensively: Heike Bickeböller, Eberhard Bodenschatz, Wolfgang Brück, Alexander Ecker, Theo Geisel, Ramin Golestanian, Helmut Grubmüller, Reinhard Jahn, Norbert Lossau Simone Scheithauer.

Supplementary materials

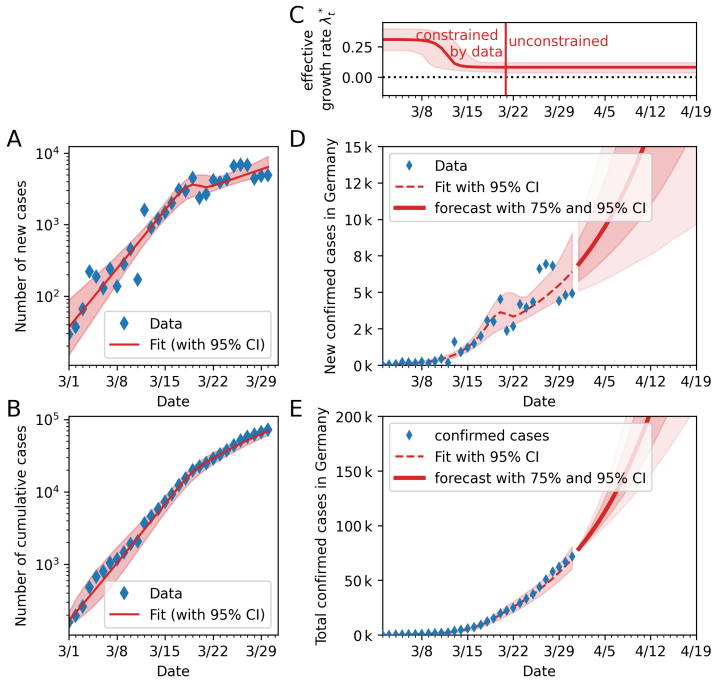

Figure 5: Inferring (the time of) the changing point in spreading rate λ, assuming only one change point. **A:** Comparison of daily recorded new cases and the model, log scale. **B:** Comparison of total recorded cases and the model, log scale. **C:** Time-dependent model-estimate of the spreading rate λ_t. **D:** Model forecast of new cases, based on the inferred λ_t, linear scale. **E:** Model forecast of total cases, based on the inferred λ_t, linear scale.

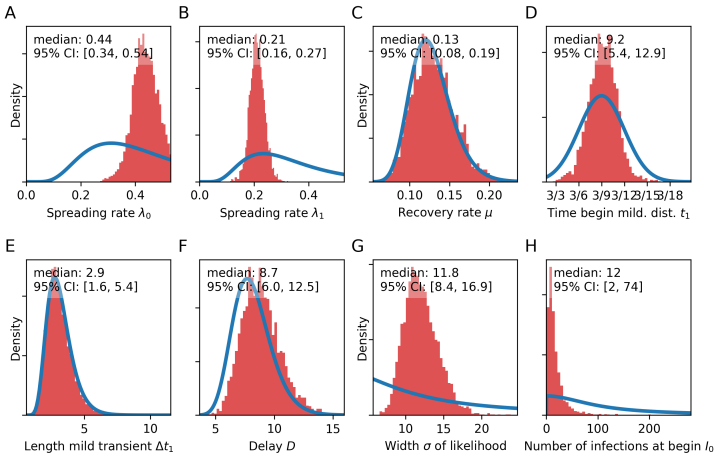

Figure 6: Posterior distributions from the change-point detection with 1 change point compared to prior distributions.

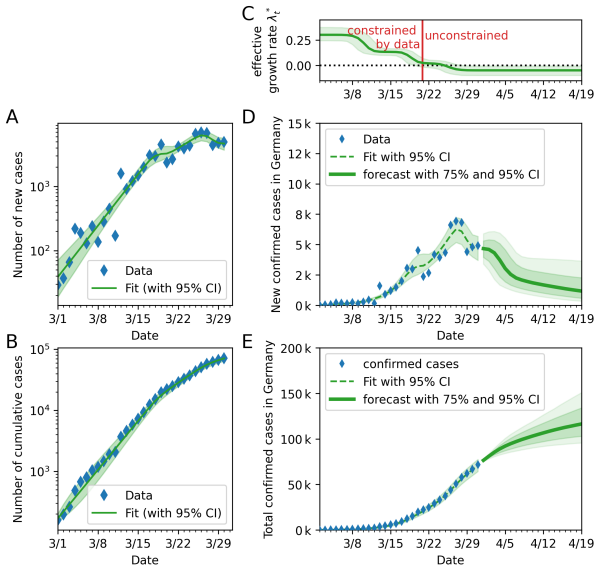

Figure 7: Inferring and forecasting (the time of) the changing point in spreading rate λ, assuming three change points. **A:** Comparison of daily recorded new cases and the model, log scale. **B:** Comparison of total recorded cases and the model, log scale. **C:** Time-dependent model-estimate of the spreading rate λ_t. **D:** Model forecast of new cases, based on the inferred λ_t, linear scale. **E:** Model forecast of total cases, based on the inferred λ_t, linear scale.

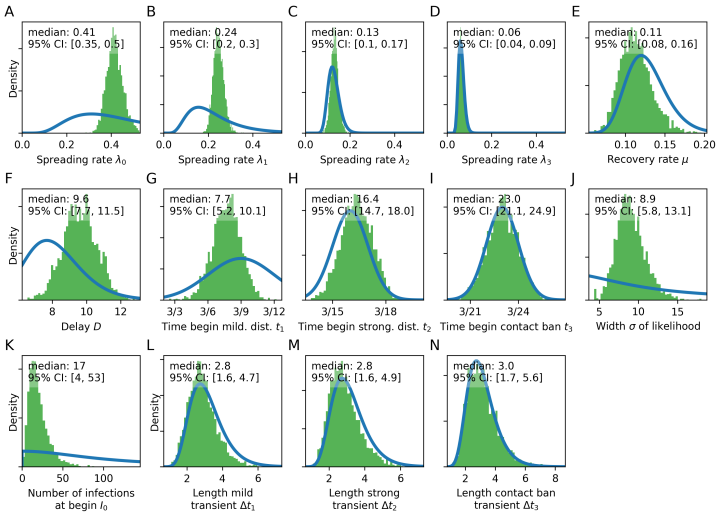

Figure 8: Posterior distributions from the change-point detection with 3 change points compared to prior distributions.